Polarization effects in autoionization processes: The $5d5g$ states in barium

E. Luc-Koenig,[1] M. Aymar,[1] R. Van Leeuwen,[2] W. Ubachs,[2] and W. Hogervorst[2]
[1]*Laboratoire Aimé Cotton, CNRS II, Bâtiment 505, 91405 Orsay Cedex, France*
[2]*Department of Physics and Astronomy, Laser Centre Vrije Universiteit Amsterdam, De Boelelaan 1081, 1081 HV Amsterdam, The Netherlands*
(Received 2 February 1995)

Accurate measurements of the autoionization widths of $5d5g$ levels of barium coupled to theoretical calculations, based on the eigenchannel R-matrix method and the multichannel quantum-defect theory, permit an investigation of the quadrupolar autoionization mechanism. The direct polarization of the inner electron by the outer one is an important correction to the Coulomb repulsion that causes autoionization. Also, the dielectronic polarization interaction significantly influences the autoionization widths. The occurrence of these polarization effects in the $5d5g$ doubly excited states with nonoverlapping valence electrons results in a significant narrowing of their widths and explains the failure of the "single-configuration model" for high-l Rydberg levels.

PACS number(s): 32.80.Dz, 32.80.Fb, 31.50.+w

I. INTRODUCTION

In recent years much attention has been paid to autoionization processes in alkaline-earth-metal atoms, both experimentally and theoretically, as they provide reliable information on intra-atomic interactions. The application of isolated-core excitation and Stark switching techniques enabled the excitation of alkaline-earth-metal atoms in autoionizing states $n_2l_2n_1l_1$ with two highly excited electrons, the outer one with relatively large angular momentum l_1 [1–4]. Due to the centrifugal barrier effect, which prevents the outer electron from penetrating in the volume taken by the inner electron and the closed-shell doubly charged core, the autoionization rate may become very low. Modern high-resolution laser techniques permit an accurate determination of these autoionization widths which then may be confronted with models describing such autoionization processes.

For states with nonoverlapping valence electrons a simplified theoretical treatment is valid and the so-called "single-configuration model for autoionization of the high-l Rydberg states" has been developed [5–7]. This model has been used to reproduce in a satisfactory way the experimental autoionization widths for the $6pnl$ levels of barium and the $5pnl$ levels of strontium [5,6] for which autoionization mainly occurs through dipolar interaction. Several refinements have been introduced to improve the description of the shorter-range quadrupolar interaction [8].

The recent measurement of autoionization widths of various $5d5g$ levels of barium located below the $5d_{3/2}$ threshold provided an ideal example to test the validity of the "single-configuration model" for autoionization of levels decaying through quadrupolar interaction [9]. Indeed it is a well-defined situation, in which there is virtually no overlap between $5d$ and $5g$ wave functions. The levels are almost purely $jl[K]$ coupled and each $5d_{j_2}5g[K]J$ level autoionizes into a single $6s_{1/2}\varepsilon l[K]J$ continuum with the same K and J values ($\mathbf{K}=\mathbf{j}+1$). Due to a negligible contribution of the exchange electrostatic interaction, the two levels $J=K\pm\frac{1}{2}$ belonging to the same jK doublet have almost identical width. Furthermore, the ejected electron has angular momentum $l=2$, 4, or 6 for K respectively equal to $(\frac{3}{2}, \frac{5}{2})$, $(\frac{7}{2}, \frac{9}{2})$, or $(\frac{11}{2}, \frac{13}{2})$. Although all the assumptions made in the model appear to be justified, the calculated autoionization widths are systematically a factor of 5 larger than the experimental data. To elucidate the origin of such discrepancies additional high-resolution experiments have been carried out resulting in an accurate determination of the autoionization widths for almost all $jl[K]$ doublets of the $5d5g$ configuration. For the study of the narrow $K=\frac{3}{2}$ and $\frac{5}{2}$ components experiments with a narrow-band pulsed-dye-amplifier system were performed, whereas the $K=\frac{11}{2}$ component, decaying into the $6d\varepsilon i$ channel, was investigated using two-photon infrared excitation. Simultaneously more elaborate theoretical calculations were executed. Correlation effects are accounted for in the framework of the eigenchannel R-matrix and multichannel quantum-defect theory (MQDT) formalisms [10–12]. The theoretical values agree rather well with experimental data. Furthermore, the detailed analysis of various models demonstrates that, in order to reproduce the experimental values, it is absolutely necessary to account for the polarization of the inner valence electron by the outer one. Also the interaction of one valence electron with the dipole induced in the doubly charged closed-shell core by the second valence electron, the so-called dielectronic polarization interaction, results in a significant contribution to the autoionization widths.

The present paper is organized as follows. The experimental developments are presented in Sec. II. In Sec. III, the main assumptions underlying the single-configuration model are summarized; then the eigenchannel R-matrix and MQDT methods, which more precisely account for correlation effects, are briefly described. The theoretical results are presented and discussed in Sec. IV.

II. EXPERIMENT

In Fig. 1 the relevant energy levels for the two-step pulsed laser excitation of autoionizing $5d_{j_2}5g[K]$ J states of barium are shown. The $K=\frac{3}{2}$ and $\frac{5}{2}$ states were populated in a resonant excitation scheme from metastable $6s5d\ ^3D$ states via intermediate $5d6p\ ^3P$ states. The experimental method to determine the autoionization widths of the $K=\frac{3}{2}$ and $\frac{5}{2}$ states is similar to the one used for excitation of $K=\frac{7}{2}$ and $\frac{9}{2}$ states which was described earlier [9]. These latter states were populated in a sequential two-photon excitation using two pulsed dye lasers. A recorded spectrum is shown in Fig. 2. The bandwidth of the laser applied for the second step determined the instrumental bandwidth of 0.07 cm^{-1}. This was sufficient to determine the widths of the $K=\frac{7}{2}$ and $\frac{9}{2}$ states that decay into $6s\varepsilon g$ continua but not for the narrow $K=\frac{3}{2}$ and $K=\frac{5}{2}$ states that decay into $6s\varepsilon d$ continua.

The feature in the present experiment that we used is for the $5d6p \rightarrow 5d5g$ transitions, narrow-band laser light produced by pulsed-dye-amplification of the output of a clockwise (CW) ring dye laser. This laser system has a resolution sufficiently high to determine the autoionization width of the narrow $K=\frac{3}{2}$ and $\frac{5}{2}$ states. Its bandwidth (0.004 cm^{-1}) and frequency profile were determined experimentally using étalons. The $5d5g$ states were excited in a collimated atomic beam, reducing the Doppler width to 0.001 cm^{-1}. The $6s5d \rightarrow 5d6p$ transitions in the wavelength range 602–611 nm were induced with a pulsed dye laser with 0.07 cm^{-1} bandwidth. To avoid line-broadening effects due to coherent two-photon excitation the two 5 ns laser pulses were separated in time by 12 ns and the laser powers were reduced to typically 0.1 μJ/pulse for both steps. At these low intensities saturation effects were clearly absent and almost no Ba^+ background signal could be recorded. For frequency calibration purposes, absorption spectra of I_2 and étalon markers (free spectral range = 149 MHz) were recorded simultaneously with the $5d5g$ spectra using a small fraction of the CW laser light. An example is shown in Fig. 3.

The $5d5g$ $[\frac{11}{2}]$ $J=5$ states, which decay into $6s\varepsilon i$ continua, could not be excited from the $5d6p\ ^3F_4$ state [9]. To populate the $K=\frac{11}{2}$ and $\frac{13}{2}$ states of the $5d5g$ configuration in a resonant excitation scheme via $5d4f$ intermediate states, the generation of infrared radiation (3.6 μm) is required. Instead we used a nonresonant two-photon excitation scheme starting out from the metastable $5d^2\ ^3F_{3,4}$ states. The $5d^2$ metastable states are populated in a low-voltage discharge with an estimated efficiency of 10^{-4}, which is two orders of magnitude lower than for metastable $6s5d$ states. For the two-

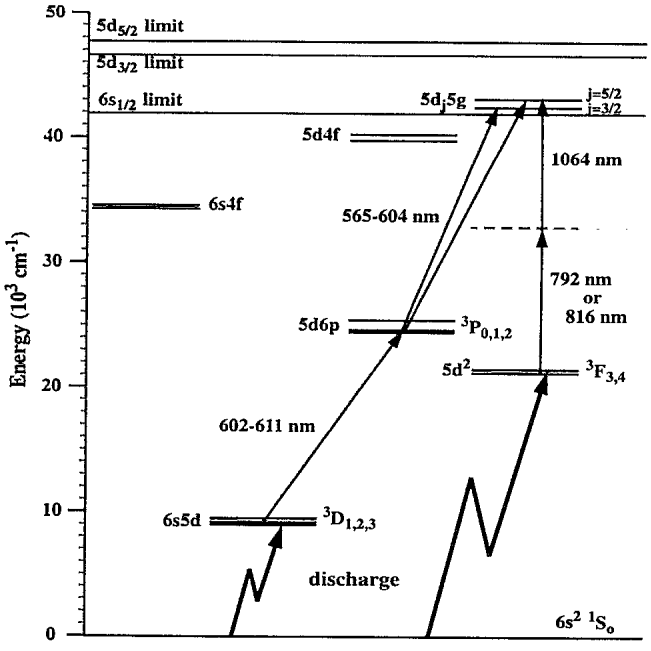

FIG. 1. Energy-level diagram showing the two-step excitation scheme probing $5d5g$ states. in the scheme on the left, sequential two-photon absorption is employed with nontemporally overlapping low-power laser pulses. In the scheme on the right, a coherent two-photon transition is induced with temporally overlapping high-power laser pulses.

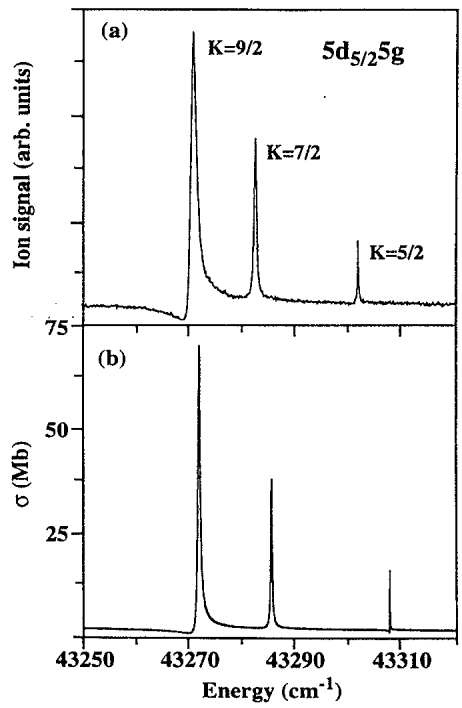

FIG. 2. Excitation spectrum $5d6p\ ^3F_4 \rightarrow 5d_{5/2}5g$ $[K=\frac{9}{2}, \frac{7}{2}$, and $\frac{5}{2}]$ in barium. The energy (in cm^{-1}) refers to the ground level $6s^2\ ^1S_0$. (a) Experimental spectrum. The bandwidth of the second laser is equal to 0.07 cm^{-1}. Note that transitions in this overview spectrum are somewhat saturated. The autoionization widths were determined from spectra taken at reduced laser power. (b) Theoretical cross section (in Mb) obtained by using the largest basis set described in the text. The dielectronic polarization term [Eq. (3)] is introduced in the Hamiltonian, and the polarization correction [Eq. (4)] is added to the electric dipole transition operator in the length form. The theoretical cross section has been convoluted with a Gaussian profile with a bandwidth equal to 0.07 cm^{-1}.

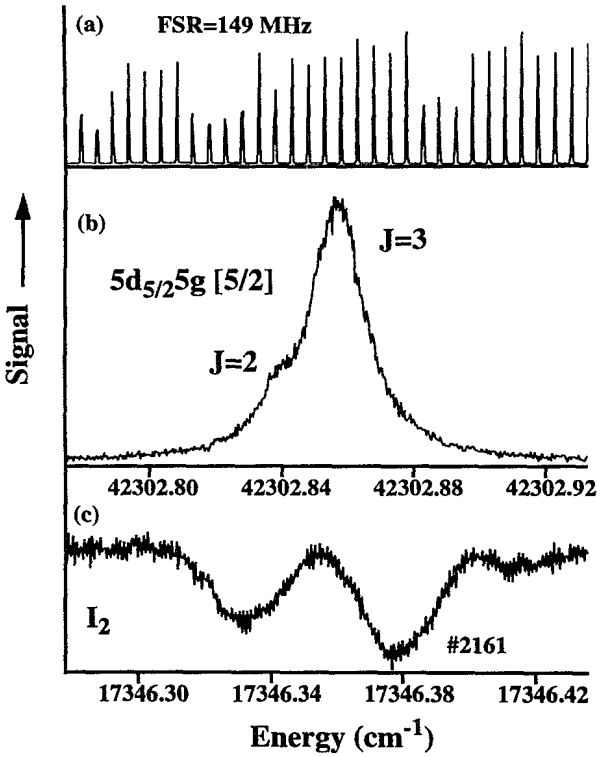

FIG. 3. Experimental recording of the $5d6p\ ^3P_2 \rightarrow 5d_{5/2}5g$ [$K=\frac{5}{2}$] transition in barium exhibiting the partially resolved levels $J=2$ and 3. (a) Etalon markers for relative frequency calibration. (b) Ba spectrum; energy scale (in cm^{-1}) with respect to the $6s^2\ ^1S_0$ ground level. (c) I_2-absorption spectrum used for absolute frequency calibration: energy scale represents the frequency of the pulsed-dye-amplification laser (bandwidth 0.004 cm^{-1}).

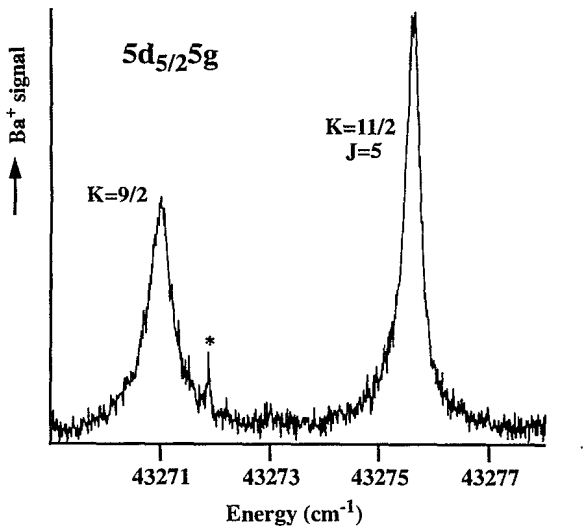

FIG. 4. Experimental recording of the $5d^2\ ^3F_3 \rightarrow 5d_{5/2}5g$ coherent two-color two-photon transition in Ba. The $K=\frac{11}{2}$ line consists of a single $J=5$ component, whereas the $K=\frac{9}{2}$ line may be composed of $J=4$ and $J=5$ components. The weak transition marked by an * is most likely a two-color two-photon transition from the $5d^2\ ^1G_4$ level to a $5d_{3/2}24g$ state.

photon transition we used IR light (1064 nm) with a pulse energy of 200 mJ, generated by an injection seeded neodymium-doped yttrium aluminum garnet (Nd:YAG) laser (bandwidth 0.003 cm^{-1}), and the output of a pulsed dye laser which was pumped by the frequency-doubled output of the same Nd:YAG laser. Styryl dyes were used to generate the required wavelengths around 800 nm with a pulse energy of 20 mJ. The two laser pulses were spatially and temporally overlapped in the interaction region. To create a large interaction volume the laser beams were unfocused and high laser powers had to be used to induce coherent two-photon transitions to $5d5g$ states. In Fig. 4 a recorded spectrum is shown. We also observed additional transitions between metastable $6s5d$ states and other bound states. These transitions could be used for energy calibration and to determine the bandwidth (0.13 cm^{-1}) and frequency profile of the dye laser.

The autoionization widths of the $5d5g$ states were determined from observed linewidths by deconvoluting the experimentally determined laser profile from the excitation spectra.

III. THEORETICAL MODELS FOR AUTOIONIZATION WIDTHS OF RYDBERG LEVELS

A. The "single-configuration autoionization model" of Nikitin-Ostrovsky and Poirier for high-l Rydberg states

The basic formalism describing autoionization of alkaline-earth-metal atoms with the inner valence electron weakly excited and the other one in a high Rydberg state with large-angular momentum has been published in several papers [5–8]. Its application to the autoionization widths of the $5dng$ levels of barium is discussed in great detail elsewhere [9]. Doubly excited levels are represented by single-configuration wave functions $n_2l_2n_1l_1$. The Rydberg electron n_1l_1 does not overlap with the valence electron n_2l_2 and is represented by a pure hydrogenic function. The line broadening associated with autoionization of this level into the $n_0l_0\varepsilon l$ continuum is calculated by perturbation theory using Fermi's golden rule and a multipole expansion of the Coulomb electron-electron interaction. In the "long-range approximation" [8] the exchange autoionization amplitude may be neglected and in the direct contribution the bielectronic Slater integral is expressed as the product of two one-electron matrix elements. One concerns the inner valence electron and the second one involves a bound-free transition matrix element for the Rydberg electron. The doubly excited levels are described in jj- or jK-coupling schemes, which are more realistic than the LS scheme. Polarization of the closed-shell core by both excited electrons can be reliably taken into account in the adiabatic approximation through the introduction of a properly screened matrix element for the valence electron [6].

B. Autoionization widths deduced from the eigenchannel R matrix plus MQDT formalism

Eigenchannel R-matrix calculations in combination with the MQDT formalism have been successfully used

to describe autoionizing spectra of alkaline-earth-metal atoms [10–12]. A finite reaction volume with radius r_0 is defined in which electron correlations must be treated in a nonperturbative way. Escape of a single electron from this volume is then described in the framework of MQDT thereby neglecting all channel interactions for $r > r_0$. Disregarding the long-range multipole interactions outside the reaction volume limits the applicability of this method to the analysis of Rydberg series $n_2 l_2 n_1 l_1$ converging toward the lowest nondegenerate ionization thresholds $n_2 l_2$ and with not too high angular momentum for the outer electron, typically $l_1 \leq 6$ [13]. For a given J value and at each energy E the jj-coupled wave functions describing the pair of electrons outside the Ba^{2+} core are determined variationally within the reaction volume using the eigenchannel R-matrix method. For this purpose a model Hamiltonian is introduced (in a.u.):

$$H = T(1) + V(r_1) + V_{so}(1) + T(2) + V(r_2) + V_{so}(2) + 1/r_{12} + V_{pol,d}(1,2) , \quad (1)$$

where 1 and 2 refer to electrons 1 and 2 whose positions are r_1 and r_2. T denotes the kinetic energy and V_{so} represents the spin-orbit interaction. V is an l-dependent electron-ionic core effective potential including an analytical term for the mean electrostatic interaction and an additional term $V_{pol,s}$ given by

$$V_{pol,s}(r) = -\tfrac{1}{2}(\alpha_d / r^4) W(l,r) . \quad (2)$$

$V_{pol,s}$ represents the polarization energy of the core in the electric field created by the *single* valence electron; α_d, fixed at 11.4 [14], is the static dipole polarizability of the core and W is an l-dependent cutoff function. The empirical parameters occurring in $V(r)$ are adjusted to obtain optimum agreement with the known spectrum of Ba^+ [12].

In Eq. (1), the interaction between the two valence electrons is given by the electrostatic term $1/r_{12}$ and by the *dielectronic* polarization correction $V_{pol,d}(1,2)$; this latter term, calculated between $l_1 l_2$ and $l_1' l_2'$ basis functions, is given by [15]

$$V_{pol,d}(1,2) = -\alpha_d (C^{(1)}(1) \cdot C^{(1)}(2)) \, (r_1 r_2)^{-2} \times [W(l_1,r_1) W(l_1',r_1) W(l_2',r_2) \times W(l_2',r_2)]^{1/4} . \quad (3)$$

$C^{(1)}(i)$ is the spherical harmonic operator of rank 1 depending on the angular coordinates of electron i and the dot denotes the scalar product of the two operators $C^{(1)}$. $V_{pol,d}$ represents the interaction of each valence electron with the dipole moment induced in the doubly charged core by the other valence electron [16–18].

The chosen two-electron basis functions describe the MQDT channels, involving open and weakly closed ones, in which one electron can escape from the reaction volume. In addition "strongly closed" channels, where both electrons are confined within the reaction volume, are added; these channels are necessary to include various relaxation and polarization effects for the inner electron perturbed by the outer one [19].

MQDT techniques [20] are used to describe the system outside the reaction volume and to calculate observables, in particular the partial photoionization cross sections $\sigma(E)$ for the various $5d6p\,^{2S+1}L_{J'} \rightarrow J$ one-photon excitation processes. In this calculation, the wave function describing the lower level is completely confined within the reaction volume. The electric dipole moment is calculated in the length formulation. Core-polarization corrections are accounted for by describing the $l \rightarrow l'$ excitation by the operator [21]

$$\mathbf{r}_{pol} = \mathbf{r}\{1 - (\alpha_d / r^3)[W(l,r) W(l',r)]^{1/2}\} . \quad (4)$$

The energy dependence of $\sigma(E)$ calculated on a fine energy mesh presents resonance structures associated with the doubly excited levels $5d5g$. Identification of the resonances follows from the analysis of the contribution of each closed channel to the wave functions. The resonant peak positions give the energy of the levels and the autoionization widths follow from the linewidths. The energy positions and widths of autoionizing levels can also be derived independently of the excitation pathway by analyzing the resonance structures exhibited by the energy dependence of the density of states in the closed channels $5d_{j_2} n_1 l_1 j_1$ as described in Ref. [13]. This procedure is used for levels with high K values which could not be excited from $5d6p$ levels.

Another way to directly determine the autoionization widths of the well isolated $5d5g$ resonances is to use, as in previous works [13,22], the "phase-shifted" MQDT parameters [23] determined from the R-matrix calculation.

In the present work r_0 must be larger than 35 a.u. as the ng orbitals are affected by centrifugal barrier effects. Furthermore, to avoid the introduction of strong energy dependence in the MQDT parameters by confinement of $5d5g$ levels within the reaction volume [15], r_0 must be less than 50 a.u. A value $r_0 = 40$ a.u. was chosen. It has been verified that for the broad levels with $K \geq \frac{7}{2}$, a value $r_0 = 35$ a.u. gives identical results (difference smaller than 0.05 cm^{-1}). This demonstrates the convergence of the R-matrix calculations. For the very narrow levels with $K \leq \frac{5}{2}$ autoionizing into the $6s\varepsilon d_{j_1}$ continuum (widths smaller than 0.1 cm^{-1}) the same uncertainty is expected, which is then almost equal to the values of the widths. To analyze the autoionization processes in the $5d5g$ levels of barium the open channels are $6s_{1/2}\varepsilon l_1 j_1$ and the weakly closed ones are restricted to the $5d_{j_2} n_1 l_1 j_1$ channels. The $6p_{j_2} np_{j_1}$ channels are treated as "strongly closed" independently of the J value. Treating them as "weakly closed" channels will result in a strong energy dependence of MQDT parameters, the $6p^2$ doubly excited levels being completely confined within the reaction volume for $r_0 \geq 35$ a.u. The $6p^2$ and $6p7p$ configurations lie far apart from the $5dng$ ones, respectively, below the $6s_{1/2}$ threshold and above the $5d_{5/2}$ threshold [24], and it is sufficient to account for the global $5dng$-$6pnp$ channel coupling. All $6pnf$ $J = 1-5$ levels are located at least 8000 cm^{-1} above the $5d_{5/2}$ threshold [25], therefore the $6p_{j_2} nf_{j_1}$ channels are "strongly closed" in the studied energy range.

IV. RESULTS AND DISCUSSION

A. Experimental results

The experimentally determined autoionization widths for various $5d_{j_2}5g$ $[K]$ J levels are collected in column 3 of Table I. For each level the corresponding decay channel is indicated in column 2. The results for $K=\frac{7}{2}$ and $\frac{9}{2}$ were already published before [9]. In this former experiment, the autoionization width of each state $5d_{j_2}5g$ $[K]$ was found to be independent of the value of J. Also no evidence for energy splittings between the two J components of a K doublet was found within the experimental resolution.

The autoionization widths of the narrow $5d5g$ states with $K=\frac{3}{2}$ and $\frac{5}{2}$ were determined using the narrow-band laser setup described in Sec. II. We measured seven transitions in a sequence $6s5d\,^3D_J \rightarrow 5d6p\,^3P_{J-1} \rightarrow 5d_{j_2}5g$ $[K]$ and all transitions showed Lorentzian line profiles. In most transitions only a single J component of a K doublet was excited due to the $\Delta J=0, \pm 1$ selection rule or to a dominant oscillator strength for one of the two J components. Only for the $5d6p\,^3P_2 \rightarrow [5d_{5/2}5g]K=\frac{5}{2}$ transition was a doublet observed as is shown in Fig. 3. The energy splitting, equal to 0.020(1) cm^{-1}, is smaller than the autoionization widths and therefore the doublet is not completely resolved. The width of the weaker $J=2$ component could be determined from the excitation spectrum from the $5d6p\,^3P_1$ level, while the width of the stronger $J=3$ component was determined by fitting the experimental profile of Fig. 3 to a doublet with a fixed value for the width of the $J=2$ component. A significant difference in the widths of the two J components of each $K=\frac{3}{2}$ and $\frac{5}{2}$ state is observed.

TABLE I. Observed and calculated autoionization widths (in cm^{-1}) for the $5d5g$ levels of barium with $J \leq 6$. (1) Identification $5d_j5g$ $[K]$ J of the $jl[K]$ coupled levels. (2) Continuum electron εl for the decay channel $6s\varepsilon l$. (3) Experimental results. The values already published in Ref. [9] are indicated with *. (4) Theoretical results deduced from the "long-range" approximation in the "single-configuration" model published in Ref. [9]. (5) R-matrix calculation disregarding the polarization of the inner valence electron: basis sets $6snl+5dnl$. (6) R-matrix calculation including the direct polarization of the inner valence electron by the Rydberg electron, but disregarding the dielectronic polarization interaction [Eq. (3)]: largest basis set. (7) R-matrix calculation including the direct polarization of the inner valence electron by the Rydberg electron and the dielectronic polarization interaction [Eq. (3)]: largest basis set.

(1)			(2)	(3)	(4)	(5)	(6)	(7)
j	K	J	εl					
$5d_{3/2}$	$\frac{5}{2}$	2	εd	0.062(4)	0.0074	0.077	0.072	0.018
$5d_{3/2}$	$\frac{5}{2}$	3	εd	0.056(5)	0.0074	0.048	0.046	0.025
$5d_{3/2}$	$\frac{7}{2}$	3	εg	0.34(3)*	1.96	2.34	0.12	0.34
$5d_{3/2}$	$\frac{7}{2}$	4	εg	0.34(3)*	1.96	2.41	0.12	0.33
$5d_{3/2}$	$\frac{9}{2}$	4	εg	0.18(2)*	1.00	1.11	0.11	0.23
$5d_{3/2}$	$\frac{9}{2}$	5	εg	0.18(2)*	1.00	1.19	0.11	0.23
$5d_{3/2}$	$\frac{11}{2}$	5	εi		2.90	3.19	1.44	1.74
$5d_{3/2}$	$\frac{11}{2}$	6	εi		2.90	3.20	1.44	1.73
$5d_{5/2}$	$\frac{3}{2}$	1	εd	0.046(3)	0.012	0.038	0.066	0.041
$5d_{5/2}$	$\frac{3}{2}$	2	εd	0.057(4)	0.012	0.077	0.061	0.025
$5d_{5/2}$	$\frac{5}{2}$	2	εd	0.0107(15)	0.0041	0.025	0.023	0.008
$5d_{5/2}$	$\frac{5}{2}$	3	εd	0.0174(23)	0.0041	0.017	0.021	0.013
$5d_{5/2}$	$\frac{7}{2}$	3	εg	0.29(3)*	1.43	1.61	0.13	0.29
$5d_{5/2}$	$\frac{7}{2}$	4	εg	0.29(3)*	1.43	1.73	0.13	0.31
$5d_{5/2}$	$\frac{9}{2}$	4	εg	0.43(4)*	2.29	2.57	0.22	0.48
$5d_{5/2}$	$\frac{9}{2}$	5	εg	0.43(4)*	2.29	2.71	0.22	0.48
$5d_{5/2}$	$\frac{11}{2}$	5	εi	0.28(3)	0.45	0.56	0.25	0.30
$5d_{5/2}$	$\frac{11}{2}$	6	εi	0.32(3)	0.45	0.55	0.25	0.30
$5d_{5/2}$	$\frac{13}{2}$	6	εi		3.37	3.95	1.83	2.15

The $5d_{5/2}5g$ $K=\frac{11}{2}$ level is recorded in coherent two-color two-photon excitation processes from the $5d^2\,^3F_3$ and $^3F_4$ levels as described in Sec. II. The excitation spectrum from the $5d^2\,^3F_3$ state at 21 250.17 cm^{-1} is shown in Fig. 4. Only the $J=5$ component of the $K=\frac{11}{2}$ state at 43 275.60(15) cm^{-1} could be excited from a $J=3$ state. The $K=\frac{9}{2}$, $\frac{7}{2}$, and $\frac{5}{2}$ states could also be observed and were found at the expected energy positions. Unfortunately we could not observe the broader $5d_{5/2}5g$ $[\frac{13}{2}]$ and $5d_{3/2}5g$ $[\frac{11}{2}]$ levels. The $5d_{5/2}5g$ $K=\frac{9}{2}$ and $K=\frac{11}{2}$ states could also be observed in excitation from the $5d^2\,^3F_4$ state (at 21 623.75 cm^{-1}). The $K=\frac{11}{2}$ state was found with the same width (within error bars) as in excitation from $5d^2\,^3F_3$. However, the energy splitting between the $K=\frac{9}{2}$ and $\frac{11}{2}$ states was found to be 0.12(3) cm^{-1} smaller than in the spectrum of Fig. 4. From this we conclude that in excitation from the $5d^2\,^3F_4$ state predominantly the $J=6$ component of the $K=\frac{11}{2}$ doublet is observed.

B. Theoretical results and discussion

The cross sections for excitation from various $5d6p\,^{2S+1}L_J$ levels were calculated using the method described in Sec. III B. Autoionization widths are determined from the linewidths of resonant peaks occurring in the energy dependence of the calculated cross sections or densities of states. These values perfectly agree with those calculated at the energy of the resonances from the "phase-shifted" MQDT parameters. To compare the theoretical spectra to the experimental ones, the calculated spectra are convoluted with a Gaussian function accounting for the laser bandwidth. This convolution is indispensable to reproduce the relative intensities of the lines, especially for those components with a width smaller than the laser width. These calculations were performed using the total Hamiltonian [Eq. (1)] with the $V_{\mathrm{pol},d}$ term [Eq. (3)] and including in the dipole transition operator the polarization correction [Eq. (4)]. For each J value the basis set includes, besides the $6s\varepsilon l$ and $5dnl$ MQDT channels, a large number of "strongly closed" channels in which the inner electron is described by n_2l_2 orbitals with $0\le l_2\le 7$ and up to seven different n_2 values. For $J=6$ this large basis set includes 1850 functions. A comparison concerning the excitation of the $5d_{5/2}5g$ $[K]$ J levels from the $5d6p\,^3F_4$ level is shown in Fig. 2; excitation of the $5d5g$ levels results from the mixing of $5d4f$ components into the lower $5d6p\,^3F_4$ level. The theoretical spectrum reproduces the experimental spectrum very well, especially the Fano profiles observed for the $K=\frac{9}{2}$, $J=5$ structure and, to a lesser extent, for $K=\frac{5}{2}$, $J=3$. These asymmetrical profiles result from the presence of $6s4f$ components in the $5d6p\,^3F_4$ wave function allowing for the direct excitation of the $6s\varepsilon d$ and $6s\varepsilon g$ continua. The deviations between the energy positions for the measured and calculated resonances (≤ 4.9 cm^{-1}) correspond to a small error ($\le 2.8\times10^{-3}$) in the calculated quantum defects with respect to the $5d_{5/2}$ limit. Such a discrepancy is not surprising because the lowest-lying states in a Rydberg series, such as the $5d5g$ states, are generally correlated and therefore more difficult to describe precisely.

To analyze the influence of various correlation effects on the $5d5g$ widths, several R-matrix calculations were carried out, using different approximations to describe the electronic interactions and introducing smaller or larger basis sets in the variational calculation.

In the simplest model, relaxation and polarization of the inner valence electron due to the outer one are completely disregarded. Only radial corrections to the monoelectronic wave functions due to core-polarization effects are accounted for by introducing the $V_{\mathrm{pol},s}$ interaction [Eq. (2)] in the effective potential experienced by the valence electrons. Here the basis sets are restricted to $6s_{1/2}n_1l_1j_1$ and $5d_{j_2}n_1l_1j_1$ functions, with the $6s_{1/2}$ and $5d_{j_2}$ wave functions describing the Ba^+ ion. With these small sets, including no more than 135 functions, direct autoionization is due only to the $5d$-$6s$ quadrupolar coupling. At this stage, there is no contribution from the dielectronic polarization correction $V_{\mathrm{pol},d}$ which only couples inner electron wave functions when $l_2'=l_2\pm1$. The calculated widths are reported in column 5 of Table I. For levels with $K\ge\frac{7}{2}$, these values are almost identical to the results reported in column 4, calculated by Van Leeuwen, Ubachs, and Hogervorst [9] using the model of Nikitin-Ostrovsky and Poirier. The $5dng$-$5dnl$ ($l=0$ or 2) channel mixing is completely disregarded in the "single-configuration model" but is accounted for in this simple R-matrix calculation. The small differences between the values reported in columns 4 and 5 demonstrate that the $5dng$-$5dnl$ channel mixing does not contribute significantly to the autoionization widths of the $5d5g$ levels. The widths calculated from this simple model are about 5–6 times larger than the experimental values although almost all assumptions made in the "long-range approximation of the single-configuration autoionization model" appear to be justified as discussed elsewhere [9]. We have checked numerically that the assumptions used in this model—factorization of the Slater integral $R^K(5d,5g;6s;\varepsilon l)$ and description of the $5g$ and εl orbitals by hydrogenic functions—are valid for $l\ge4$. For $l<4$, neither the factorization nor the use of hydrogenic orbitals remains valid, owing to the strongly nonhydrogenic behavior of the εl orbitals and their significant overlap with the $5d$, $5g$, and $6s$ orbitals. From this it follows that the single-configuration model is not expected to reproduce the autoionization widths of the $5d5g$ levels with $K\le\frac{5}{2}$.

In a more realistic calculation relaxation and polarization of the inner electron by the outer one are taken into account in the variational calculation by adding to the basis set the large number of strongly closed channels described above. In the Hamiltonian, the dielectronic interaction is restricted to the electrostatic term alone, therefore the polarization of the inner valence electron is due only to the direct perturbation by the outer Rydberg electron. The corresponding autoionization widths are given in column 6 of Table I. For levels with $K\ge\frac{7}{2}$, these widths are smaller than experimental values by a factor

ranging from 1.5 to 3. For $J>3$ this decrease in width can only be ascribed to polarization effects. Indeed in the studied energy range the only weakly closed channels are the $5dnl$, all $6pnl$ channels with $l\geq 3$ being strongly closed, as the $6p4f$ configuration lies far above the $5d_{3/2}$ threshold. For $J\leq 3$ the mixing between the $5d5g$, $6p^2$, and $6p7p$ configurations, involving very large energy differences, is negligible and only the global contribution of the $6pnp$ channels is accounted for in the present calculation by treating them as strongly closed. An analysis of the eigenvectors of the Hamiltonian matrix built on only the closed basis functions, i.e., the functions vanishing at the surface of the reaction volume, demonstrates that $5d5g$ wave functions contain small components with a different angular behavior. The more significant components, of the type $6pnl$ and $4fnl$, represent the polarization of the inner electron wave function under the influence of the outer electron. For example, in the eigenvector associated with the $5d_{3/2}5g$ $[K=\frac{9}{2}]$ $J=5$ level, the weights of the $6pnl$ and $4fnl$ components are, respectively, 0.06% and 0.03%. Owing to the large strength of the dipolar interaction $6pnl$-$6s\varepsilon l'$ the $5d5g$-$6pnl$ dipolar mixing, although very small, is sufficient to strongly modify the $5d5g$ autoionization widths resulting from the weak quadrupolar coupling $5d5g$-$6s\varepsilon l$. An almost negligible contribution arises from the $5d5g$-$4fnl$ dipolar mixing, the $4fnl$ components autoionizing only through octupolar coupling.

The $5d5g$-$(6pnl+4fnl)$ mixing can result not only from dipolar contribution of the electrostatic interaction but also from the dielectronic polarization term $V_{\mathrm{pol},d}$ [Eq. (3)], which has the same angular dependence. Column 7 reports the autoionization widths determined by accounting for $V_{\mathrm{pol},d}$ keeping the same basis set as in the previous calculation. This correction increases the widths for the $K\geq\frac{7}{2}$ levels and decreases them for $K\leq\frac{5}{2}$. This correction has the opposite effect of the direct polarization of the inner electron by the outer one, which decreases the widths for the $K\geq\frac{7}{2}$ levels and increases them for $K\leq\frac{5}{2}$. This demonstrates that the dielectronic polarization correction partly compensates the polarization of the inner valence electron directly produced by the outer Rydberg electron. Indeed the dipole induced in the closed-shell core has the same orientation as the one occurring in the charge distribution associated with the inner valence electron; then their mutual interaction leads to a partial cancellation of these dipoles. These changes in the polarization are confirmed by comparing the $5d5g$ eigenvectors obtained in this model by diagonalizing the closed part of the Hamiltonian to those obtained in the previous model. For the levels with $K\geq\frac{7}{2}$ the calculated widths are in good agreement with the experimental data, the discrepancies being generally less than 0.05 cm^{-1}. It is to be emphasized that this good agreement is obtained for levels autoionizing into the $6s\varepsilon g$ or the $6s\varepsilon i$ continua. For the $K\leq\frac{5}{2}$ levels, which decay into the $6s\varepsilon d$ continua, the agreement is less satisfactory, but the corresponding widths are much smaller. Furthermore, in this case it is difficult to describe precisely the $5dng$-$6pnp$ channel coupling which significantly influences the autoionization mechanism. The crucial influence of the $5d5g$-$6pnl$ dipolar mixing on the autoionization widths of the $5d5g$ levels has been verified in a simple model including in the Hamiltonian the term $V_{\mathrm{pol},d}$, but restricting the basis set to wave functions of the type $6snl$, $5dnl$, or $6pnl$ (the dimensions of the corresponding basis do not exceed 200). The results of this model are very close to those calculated using the complete basis set. This shows that the predominant correction to the $5d5g$-$6s\varepsilon l$ quadrupolar autoionization arises from the $5d5g$-$6pnl$ dipole coupling followed by dipolar ionization $6pnl$-$6s\varepsilon l'$.

V. CONCLUSION

For the $5d5g$ levels of barium although almost all assumptions inherent in the "single-configuration autoionization model for high-l Rydberg levels" seem to be justified this model is unable to reproduce the experimental data. As a matter of fact, in the present case the autoionization decay of the $5d5g$ levels, which are nearly purely $jl[K]$ coupled, arises directly from the weak quadrupolar interaction. Consequently additional contributions, which in a perturbative treatment would appear at higher orders, may contribute significantly to the autoionization process. The present analysis shows that the direct polarization of the inner valence electron by the outer one significantly influences the autoionization mechanism. This effect corresponds to the dipolar coupling of the $5dng$ channels with predominantly $6pnl$ and $4fnl$, followed by autoionization of these latter channels. The mixing with the $6pnl$ channel is of particular importance on account of the strong dipolar interaction $6pnl$-$6s\varepsilon l'$. It is to be emphasized that this channel mixing is significant in an energy range located for $J\geq 3$ well below the position of the lowest configurations of the type $6pnl$ or $4fnl$. This important contribution of strongly closed channels is well established now [19]. Another significant contribution to the autoionization processes arises from the interaction of one valence electron with the dipole induced in the core by the other valence electron. This dielectronic core-polarization effect results in a decrease of the polarization of the inner electron. This interaction has been shown to have a significant influence on the autoionization widths in a neutral atom (its important role in the spectra of negative ions has already been demonstrated in the approach using the R-matrix method [26]). It is more favorable to analyze the contribution of polarization effects in the $5dng$ series of Ba than in the $3dng$ series of Ca or the $4dng$ series of Sr. Indeed in Ba, the $6p^2$ and $6p7p$ levels lie outside the energy range in between the $6s$ and $5d$ thresholds, while homologous levels of Ca [27,28] (Sr [29]) are located between the $4s$ and $3d$ ($5s$ and $4d$) thresholds.

Polarization effects, and especially the polarization of the inner valence electron by the outer one, remain of importance over the whole $5dng$ series. Even for relatively high n values the polarization of the inner electron by the outer one remains significant; for example, it decreases the scaled autoionization width $\Gamma\nu^3$ (ν is the effective principal quantum number) calculated for the

$5d_{5/2}10g$ $[K=\frac{9}{2}]$ doublet using the single-configuration model (30×10^{-4} a.u.) by a factor of 30 [9]. Including the dielectronic polarization effect increases this new calculated value by a factor of 4. The obtained value of 4×10^{-4} a.u. for the scaled autoionization rate of the $5d_{5/2}10g$ $[K=\frac{9}{2}]$ level is in rather good agreement with the experimental value 6×10^{-4} a.u. [9], taking into account the small value of this width.

This effect of core polarization, that is, the correlation between core and valence electrons involving the excitation of one electron outside the core has been known for a long time to affect the binding energies, term splittings, oscillator strengths, and cross sections substantially [16–18]. Much calculational effort has been invested recently in this field [30–32]. Configuration expansions including one-electron excitation from the core were used in which valence-valence correlation and core polarization were treated on an equal footing. However, these calculations are known to be of slow convergence and can be applied to the lowest-lying configurations only. This type of calculation produced evidence that correlations between valence and core electrons are especially important in case of a valence electron occupying an nl orbital belonging to the same n shell as the outer electrons of the core [31]. This situation occurs in the $5d5g$ configuration of barium where the two valence electrons have the same principal quantum number $n=5$ as the outer subshells of the ionic core. This is probably the origin of the phenomena described in the present paper.

The accurate measurement of the autoionization widths of the $5d5g$ levels of barium permits a detailed investigation of the autoionization mechanisms, leading to insights into the importance of polarization effects. In particular, the high resolution of the laser system based on pulsed-dye-amplification of the output of a CW ring dye laser permitted an accurate measurement of the resonance structures of the $K=\frac{3}{2}$ and $\frac{5}{2}$ levels. For these levels the accurate determination of the small J-dependent autoionization rates and of the energy splitting for the $5d_{5/2}5g$ $[K=\frac{5}{2}]$ doublet remain a challenge to the development of more sophisticated theoretical models.

ACKNOWLEDGMENTS

We wish to thank Kjeld Eikema for setting up the narrow-band pulsed-dye-amplification laser system and controlling it during the measurements on the low K components. We would like to thank Jean-Marie Lecomte and Pierre Camus for valuable discussions. Numerical calculations were carried out on the Cray 98 belonging to the "Institut de Développement et des Ressources en Informatique Scientifique" of the Centre National de la Recherche Scientifique and on the Cray YMPEL of the computer center "Paris Sud Informatique." The Laboratoire Aimé Cotton is associated with the Université Paris-Sud.

[1] W. E. Cooke, T. F. Gallagher, S. A. Edelstein, and R. M. Hill, Phys. Rev. Lett. **40**, 178 (1978).
[2] U. Eichmann, V. Lange, and W. Sandner, Phys. Rev. Lett. **68**, 21 (1992).
[3] L. Pruvost, P. Camus. J. M. Lecomte, C. R. Mahon, and P. Pillet, J. Phys. B. **24**, 4723 (1991).
[4] P. Camus, S. Cohen, L. Pruvost, and A. Bolovinos, Phys. Rev. A **48**, R9 (1993).
[5] S. I. Nikitin and V. N. Ostrovsky, J. Phys. B **13**, 1961 (1980).
[6] M. Poirier, Phys. Rev. A **38**, 3484 (1988).
[7] H. Van Regemorter, J. Phys. B **23**, 1797 (1990).
[8] M. Poirier, Phys. Rev. A **50**, 1335 (1994).
[9] R. Van Leeuwen, W. Ubachs, and W. Hogervorst, J. Phys. B **27**, 3891 (1994).
[10] C. H. Greene and L. Kim, Phys. Rev. A **36**, 2706 (1987).
[11] M. Aymar, J. Phys. B **23**, 2967 (1990).
[12] C. H. Greene and M. Aymar, Phys. Rev. A **44**, 1773 (1991).
[13] M. Aymar, E. Luc-Koenig, and J. M. Lecomte, J. Phys. B **27**, 2425 (1994).
[14] V. P. Shevelko and A. V. Vinogradov, Phys. Scr. **19**, 275 (1979).
[15] J. M. Lecomte, M. Telmini, M. Aymar, and E. Luc-Koenig, J. Phys. B **27**, 667 (1994).
[16] C. D. H. Chisholm and U. Opik, Proc. Phys. Soc. London **83**, 541 (1964).
[17] S. Hameed, J. Phys. B **5**, 746 (1972).
[18] D. W. Norcross, Phys. Rev. Lett. **32**, 192 (1974).
[19] K. Bartschat and C. H. Greene, J. Phys. B **26**, L109 (1993).
[20] U. Fano and A. R. P. Rau, *Atomic Collisions and Spectra* (Academic, New York, 1986).
[21] S. Hameed, A. Herzenberg, and M. G. James, J. Phys. B **1**, 822 (1968).
[22] E. Luc-Koenig, M. Aymar, and J. M. Lecomte, J. Phys. B **27**, 2447 (1994).
[23] J. M. Lecomte, J. Phys. B **20**, 3645 (1987).
[24] P. Camus, M. Dieulin, A. El Himdy, and M. Aymar, Phys. Scr. **27**, 125 (1983).
[25] M. Abutaleb, R. J. de Graaff, W. Ubachs, and W. Hogervorst, Phys. Rev. A **44**, 4187 (1991).
[26] U. Thumm and D. W. Norcross, Phys. Rev. A **45**, 6349 (1992).
[27] S. Assimopoulos, A. Bolovinos, A. Jimoyiannis, P. Tsekeris, E. Luc-Koenig, and M. Aymar, J. Phys. B **27**, 2471 (1994).
[28] E. Luc-Koenig, A. Bolovinos, M. Aymar, S. Assimopoulos, A. Jimoyiannis, and P. Tsekeris, Z. Phys. D **32**, 49 (1994).
[29] S. Goutis, M. Aymar, M. Kompitsas, and P. Camus, J. Phys. B **25**, 3433 (1992).
[30] N. Vaeck, M. Godefroid, and J. E. Hansen, J. Phys. B **24**, 361 (1991).
[31] T. Brage and C. Froese-Fischer, Phys. Scr. **45**, 43 (1992).
[32] T. Brage, C. Froese-Fischer, N. Vaeck, and M. Godefroid, Phys. Scr. **48**, 533 (1993).